

Analysis and Estimation of the Lift Components of Hovering Insects

Lance W. Traub*

Texas A&M University, College Station, Texas 77843-3141

An analysis is undertaken to provide a simple analytic expression to estimate the stroke averaged lift of a hovering insect based on geometric and kinematic data. The expression should prove useful in the conceptual design of biologically inspired microaerial vehicles. The study includes estimation of the average vortex lift developed. The leading-edge suction analogy in conjunction with actuator disk theory is invoked to establish the relationship between axial force on the wing and vortex lift. The expression allows decomposition of the total loading into its attached flow and vortex lift components. For the insects investigated the estimated vortex lift typically constituted 27–50% of the attached flow lift and approximately 23–34% of the total lift.

Nomenclature

C_L	=	stroke-averaged lift coefficient
C_{La2D}	=	lift-curve slope, two dimensional
c	=	local chord
c_r	=	wing root chord
D_i	=	induced (vortex) drag
f	=	flapping frequency
J	=	pseudo-advance ratio
K, K_{mean}	=	constant
L_{att}	=	attached flow lift
L_{attN-S}	=	attached flow lift, with zero leading-edge suction
L_{tot}	=	total wing lift
L_v	=	vortex lift
q	=	dynamic pressure
R	=	wing length
S	=	wing area
T	=	leading-edge thrust
U	=	wing translational velocity
U_{eff}	=	time-and stroke-averaged stroke plane wing velocity
w	=	average advance velocity normal to the stroke plane
w_{ave}	=	average bound vortex-induced downwash velocity
w_{bound}	=	bound vortex-induced downwash velocity
w_{vortex}	=	trailing vortex-induced downwash velocity
α_{bound}	=	angle of attack component as a result of the wing's bound vortex
α_g	=	geometric angle of attack
α_{vortex}	=	angle of attack component as a result of the wing's trailing vortex
β	=	stroke plane inclination angle
Γ	=	circulation
Γ_v	=	leading-edge vortex circulation
ε	=	delta-wing semi-apex angle
Λ_v	=	delta-wing leading-edge sweep angle
ρ	=	density
σ	=	constant, relates to the second moment of area of an insect wing
ϕ	=	stroke angle
ω	=	stroke plane wing angular velocity

Introduction

MILLIONS of years of biological optimization have culminated in insects possessing unsurpassed aerial mastery. Insects are capable of hover and a vast range of maneuvers including rapid accelerations, changes of direction, and even somersaults. Recent experimental investigations^{1,2} have greatly aided in the understanding of the mechanisms used by insects to facilitate their demonstrated aerial prowess. Weis-Fogh³ showed that some insects could not generate all of the lift over a stroke cycle that they required in the fashion employed by man-made devices, that is, through steady-state attached potential lift.

In the 1930s Winter⁴ in Germany studied the delta-wing configuration to delay the effects of compressibility (i.e., $d\rho \neq 0$) encountered in high-speed flight. A characteristic of sharp highly swept (and delta) wings is the formation of leading-edge vortices above the wing (see Fig. 1). These vortices are formed due to enforced separation of the leading-edge boundary layer of the wing. This free shear layer rolls up forming a vortex above the wing. Two-dimensional vortices are generally not stable and require axial flow along their core for stability. This is naturally effected on a delta wing. This vortex is generally beneficial as it significantly augments the lift that the wing generates by inducing high surface velocities. This lift enhancement increases as the wing becomes more highly swept or slender. These vortices are highly stable for a wing angle of attack range from 0 deg to about 30 deg (depending on the wing's slenderness).

Early work by Weis-Fogh,³ as well as recent studies by Ellington et al.² and Dickinson and Gotz,⁵ have suggested various unsteady lift generation mechanisms that can be used by insects to augment their steady-state lift production. An initial mechanism denoted the "fling" by Weis-Fogh³ consists of an insect rapidly spreading the anterior edges of its wings prior to the downstroke. The benefit of such a mechanism is that the lift on each wing builds up virtually instantly without delay from the so-called Wagner⁶ effect. This follows from Kelvin's theorem for inviscid flow ($D\Gamma/Dt = 0$) in that the total circulation of a system of particles must remain constant and leads to the formation of a starting vortex for an accelerated wing. This is achieved in the fling by each wing essentially possessing the starting circulation (vortex) for the other wing. There is, however, some experimental evidence that at low Reynolds numbers and angles of attack the Wagner effect might be absent.⁷ The fling mechanism is not, however, used by many insects. Studies of the flow over a Hawkmoth by Liu et al.⁸ have shown experimentally and computationally that this insect uses vortex-induced suction to augment the normal force on the wings. This vortex lift is generated by a vortex formed at the wing's leading edge caused by dynamic stall, that is, an eruption or separation of vorticity from the wing's leading edge that rolls up to form a coherent vortex. The vortex is strengthened during the initial part of the downstroke. This vortex is directly analogous to the leading-edge vortex over a delta wing.

Received 21 May 2001; revision received 23 June 2003; accepted for publication 6 July 2003. Copyright © 2003 by Lance W. Traub. Published by the American Institute of Aeronautics and Astronautics, Inc., with permission. Copies of this paper may be made for personal or internal use, on condition that the copier pay the \$10.00 per-copy fee to the Copyright Clearance Center, Inc., 222 Rosewood Drive, Danvers, MA 01923; include the code 0021-8669/04 \$10.00 in correspondence with the CCC.

*TEES Research Scientist/Lecturer, Aerospace Engineering Department, Associate Member AIAA.

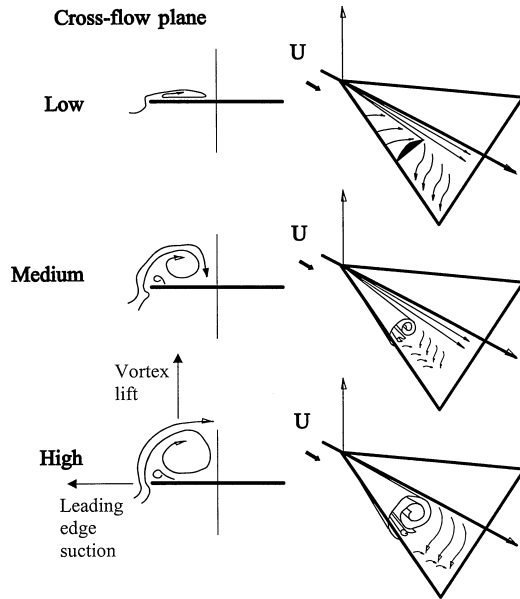


Fig. 1 Typical delta-wing flowfield at low, medium, and high angles of attack. At medium to high angles of attack, the primary vortex induces separation of the crossflow boundary layer causing the formation of a secondary vortex of opposite rotation.

As just discussed, the vortex over a delta wing is stable due to the high axial velocity component along its core. A similar effect is achieved on an insect wing by the significant spanwise pressure gradient caused by the linear variation in the wing's translational velocity ωr , where r is the local wing length. Velocities and hence pressures are highest and lowest respectively, near the wing tip. This draws the vortex outboard and on account of its axial flow stabilizes it.

The effect of the leading-edge vortices on the force on a delta wing was greatly simplified by the contribution of Polhamus⁹ in the 1960s, with the publication of his leading-edge suction analogy. Polhamus, through great intuition, surmised that the effect of the leading-edge separation was to effectively rotate the chordwise-orientated suction force to the plane of the normal force. Naturally, lift would be augmented significantly, but drag would also increase. The theory assumes that the flow reattaches inboard of the vortex for the suction to be recovered.

As discussed by Smith et al.,¹⁰ various methodologies have been developed to estimate animal performance. These techniques range from simple momentum methods to unsteady Navier–Stokes computational-fluid-dynamics simulations. None of the simpler methods calculate nonlinear loading, whereas the more complicated numerical methods do not allow easy extraction of this data, nor is it certain that the calculated data are representative. Numerical methods do not explicitly show the relationship between the generated lift and the wing geometric and kinematic properties and thus imbue less of a “feel” when data are analyzed.

It would be useful for biologists as well as engineers developing microaerial vehicles to have a simple method to estimate the amount of attached flow and vortex lift that an insect can develop and hence be able to estimate the lift (or weight) of an insect from kinematic data. Consequently, a simple method is presented that empirically combines momentum theory and Polhamus⁹ tenet to yield a relation that decomposes the lift into its components as well as provides an estimate of the total lift of the insect or microaerial vehicle from kinematic and geometrical data.

Theoretical Development

The total instantaneous lift developed by an insect can be considered to consist of an attached flow, vortex, inertial, rotational, and wake capture components. Assuming simple harmonic-type motion for wing translational (i.e., movement in the stroke plane) motions, the inertial component sums to zero over the stroke cycle, whereas

the relative magnitude and use of wake capture and rotational circulation as lift augmentation mechanisms are not firmly established. Additionally, the complexity of these processes does not readily yield analytic expressions for prediction. Time (and stroke) average considerations suggest that the attached flow and vortex lift are the major components of lift developed by an insect and will thus be considered in the following analysis.

The method presented next is limited to the case of hovering flight to allow practical realization. The time-averaged attached flow lift of an insect wing can be estimated using actuator disk theory as detailed by Ellington.¹¹ In this theory vertical application of the momentum equation and Bernoulli's equation yields

$$L_{\text{att}} = 2\rho w_{\text{ave}}^2 (R^2 \phi / 2) 2 \cos(\beta) \quad (1)$$

where β is the inclination of the stroke plane from the vertical and $R^2 \phi / 2$ is the effective area swept by each wing. Rearranging this equation to determine the average downwash through the wings gives

$$w_{\text{ave}} = \sqrt{L_{\text{att}} / 2\rho R^2 \phi \cos(\beta)} \quad (2)$$

The downwash velocity w_{ave} represents the averaged downwash induced by the wing's bound vortex system and is associated with the circulatory lift of the wing. In actuator disk theory it is assumed that the induced velocity is uniform over the swept area so as to simplify the analysis. In general, assuming a simple harmonic time-averaged motion the downwash components over the insect wing can be considered to consist of a bound and induced (vortex) components, which when combined equal the component of the freestream normal to the wing surface (see Figs. 2a and 2b). This is required to enforce the no-penetration boundary condition on the wing surface. These velocity components can be interpreted as an angle of attack by writing

$$\alpha_{\text{bound}} = w_{\text{ave}} / U_{\text{eff}}, \quad \alpha_{\text{vortex}} = w_{\text{vortex}} / U_{\text{eff}}$$

The effective velocity is the time- and stroke averaged velocity relative to the insect wing in the stroke plane and is given by $U_{\text{eff}} = \phi f R$.

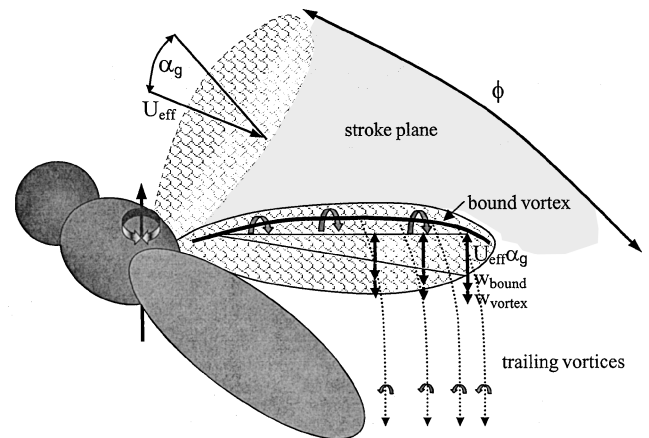


Fig. 2a Insect wing bound and trailing vortex system.

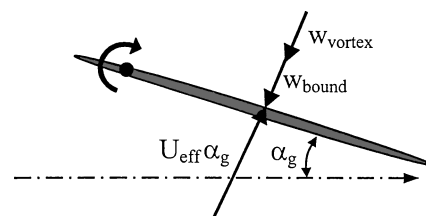


Fig. 2b Time- and stroke-averaged induced and translational velocity components seen by a translating wing.

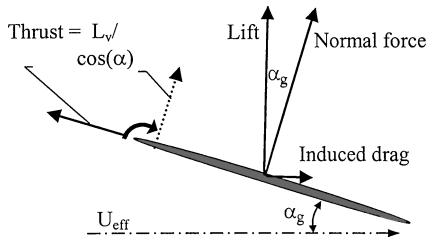


Fig. 2c Averaged loading components experienced by a translating wing. Polhamus' analogy can be seen as the rotation of the wing's leading edge thrust through 90 deg to the plane of the normal force. This results in augmentation of the normal force with a concomitant loss of the leading-edge thrust.

Thus, we can write

$$\alpha_g = \alpha_{\text{bound}} + \alpha_{\text{vortex}} \quad (3)$$

The α_{bound} component is the downwash associated with the momentum transfer required to generate the attached lift. The α_{vortex} component is the induced angle of attack caused by the trailing vortex system shed by the wing. This trailing vortex system results from changes in loading across the span of the wing; in addition, vorticity is also shed because of the change of wing velocity and incidence throughout the stroke cycle. These vorticity components are perpendicular in orientation with the vortex lines shed parallel to the trailing edge for the latter case. Combining Eqs. (2) and (3) yields an estimate of the average induced angle of attack caused by the trailing vortex system:

$$\alpha_{\text{vortex}} = \alpha_g - \sqrt{L_{\text{att}} / 2\rho R^2 \phi \cos(\beta) (1/\phi f R)} \quad (4)$$

The drag caused by the time-(and stroke-) averaged trailing vortex system can be estimated from the induced angle of attack α_{vortex} . (This drag is associated with the kinetic energy content per unit length of the wake.) The effect of α_{vortex} is to rotate the resultant force on the wing such that it has a rearward component. The vortex or induced drag is computed as

$$D_i = \alpha_{\text{vortex}} L_{\text{att}} \quad (5)$$

Thus

$$D_i = L_{\text{att}} \alpha_g - L_{\text{att}} \sqrt{L_{\text{att}} / 2\rho R^2 \phi \cos(\beta) (1/\phi f R)} \quad (6)$$

As clearly verified by Van den Berg and Ellington,¹² the lift developed by an insect is composed of both an attached component and that as a result of a vortex developed along the wing leading edge. This vortex forms as a result of a dynamic-stall mechanism following pronation. A similar vortex forms on slender swept thin wings. A method to estimate the lift resulting from these vortices was developed by Polhamus⁹ in the 1960s as already discussed. Polhamus surmised that the leading-edge suction (for attached flow) is equal to the vortex lift that the wing develops if the leading-edge flow separates and rolls up to form a coherent vortex. The total lift of the wing with vortices is then given by the sum of the vortex lift and the attached flow lift with no leading-edge suction. The effect of the vortex flow on the attached flow is not explicitly calculated. However, Polhamus' theory has been validated through comparison with experiment^{13,14} for both the magnitude of the total lift as well as that of its components.

The attached flow thrust (i.e., the inviscid axial force) can be computed as (see Fig. 2c)

$$T = L_{\text{att}} \alpha_g - D_i \quad (7)$$

which yields

$$T = L_{\text{att}} \sqrt{L_{\text{att}} / 2\rho R^2 \phi \cos(\beta) (1/\phi f R)} \quad (8)$$

Following Polhamus⁹ supposition, this force is rotated through 90 deg to the plane of the normal force (Fig. 2c). Thus the vortex lift is given by

$$L_v = \frac{L_{\text{att}}^{3/2} \cos(\alpha_g)}{\sqrt{2\rho R^2 \phi \cos(\beta)}} \left(\frac{1}{\phi f R} \right) \quad (9)$$

where L_{att} is the lift-developed assuming leading-edge suction (i.e., the flow is assumed to remain attached at the wing's leading edge).

Generally, the attached flow lift (with no leading-edge suction) can be written as the product of the dynamic pressure, the wing area, and the lift coefficient. Thus

$$L_{\text{attN-S}} = q S C_L = \frac{1}{2} \rho U^2 S C_L \quad (10)$$

The time-(and stroke-) averaged dynamic pressure and wing area can be expressed as (assuming simple harmonic oscillation of the wings)

$$q S = \rho \pi^2 f^2 \phi^2 R^3 c_r \sigma / 4 \quad (11)$$

Ellington¹¹ suggests a value of 0.49 for σ .

An appropriate (non-numerical) explicit determination of an expression yielding the average C_L is not possible, as C_L incorporates complex time-averaged three-dimensional flow effects. The lift coefficient's dependence on geometric parameters can be estimated semi-empirically using considerations from propeller theory. Generally, the lift coefficient, or more appropriately for a propeller the thrust coefficient, is dependent solely on the advance ratio, that is, the ratio of the forward flight speed (i.e., advance rate) to the blade rotational velocity. However, in the present analysis the rotor is not advancing (moving vertically), but is stationary in hover. An effective advance velocity can however be estimated to yield a pseudo-advance ratio. From no-penetration considerations (Fig. 2b) the average velocity normal to the stroke plane must be such that it balances the component normal to the wing surface as a result of the forward movement of the wings:

$$w = U_{\text{eff}} \tan(\alpha_g) \frac{2c_r R \pi / 4}{R^2 \phi} \quad (12)$$

where $2c_r R \pi / 4$ is the wing area (for an elliptic planform) and $R^2 \phi$ is the swept area; their ratio is the solidity. Thus the pseudo-advance ratio J is given by

$$J = \frac{\tan(\alpha_g) c_r \pi}{2R \phi} \quad (13)$$

or $J \propto c_r / R \phi$. It can thus be inferred that $C_L = f(J) = f(c_r / R \phi)$. Thus the attached flow lift with no leading-edge suction can be expressed as

$$L_{\text{attN-S}} = q S K (c_r / R \phi) \quad (14)$$

where the parameter K is a constant of proportionality and incorporates all time-averaged effects. Using this approach, the vortex lift [Eq. (9)] can be written as

$$L_v = \frac{[q S K (c_r / R \phi) / \cos(\alpha_g)]^{3/2} \cos(\alpha_g)}{\sqrt{2\rho R^2 \phi \cos(\beta)}} \left(\frac{1}{\phi f R} \right) \quad (15)$$

The $L_{\text{attN-S}}$ term is reduced by $\cos(\alpha_g)^2$ to account for the loss of leading-edge suction; the derivation of vortex lift assumes an attached leading-edge flow, that is, $L_{\text{att}} = L_{\text{attN-S}} / \cos(\alpha_g)^2$. The factor $1 / \cos(\alpha_g)^2$ arises as with no leading-edge suction on a flat wing; the resultant inviscid force is normal to the wing's surface. Thus the lift component (which is perpendicular to U_{eff}) is the normal force multiplied by $\cos(\alpha_g)$ (see Fig. 2b). Additionally, the component of the freestream that contributes to the normal force is perpendicular to it (the normal force) and is thus given by $U_{\text{eff}} \cos(\alpha_g)$.

Table 1 Experimental animal data from Weis-Fogh³

Animal	Weight, N	Wing length, m	Wing root chord, m	Flapping frequency, Hz	Stroke angle, rad
1 ^a	0.00001	0.0025	0.0007	600	1.83
2 ^b	0.00002	0.0030	0.0015	240	2.62
3 ^c	0.00010	0.0063	0.0016	262	2.09
4 ^d	0.00028	0.0173	0.0046	53	2.09
5 ^e	0.00056	0.0097	0.0037	159	2.09
6 ^f	0.00090	0.0132	0.0048	143	2.09
7 ^g	0.00100	0.0100	0.0043	240	2.09
8 ^h	0.00140	0.0155	0.0048	80	3.14
9 ⁱ	0.00150	0.0127	0.0048	182	2.09
10 ^j	0.00280	0.0210	0.0100	73	2.09
11 ^k	0.00480	0.0166	0.0070	143	2.60
12 ^l	0.00600	0.0243	0.0092	104	2.09
13 ^m	0.01120	0.0500	0.0230	29.1	2.09
14 ⁿ	0.01600	0.0500	0.0230	30	2.09
15 ^o	0.02120	0.0540	0.0250	27.3	2.09

^aDiptera; *Aedes aegypti*.^bDiptera; *Drosophila virilis*.^cDiptera; *Theobaldia annulata*.^dDiptera; *Tipula* sp.^eDiptera; *Calliphora erythrocephala*.^fHymenoptera; *V. vulgaris*.^gHymenoptera; *Apis mellifica*.^hColeoptera; *Cerambycid* species.ⁱDiptera; *Eristalis tenax*.^jLepidoptera; *Macroglossum stellatorum*.^kHymenoptera; *B. lapidarius*.^lHymenoptera; *Vespa crabro*.^mLepidoptera; *M. sexta*.ⁿLepidoptera; *Sphinx ligustri*.^oLepidoptera; *Manduca sexta*.

It follows that the effect of loss of leading-edge suction is to reduce the attached flow lift by $\cos(\alpha_g)^2$.

Thus the total lift of the wing is written as

$$L_{\text{tot}} = L_{\text{attN-S}} + L_v$$

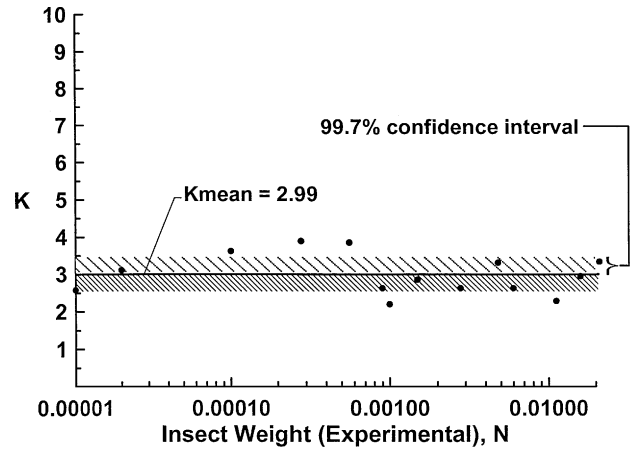
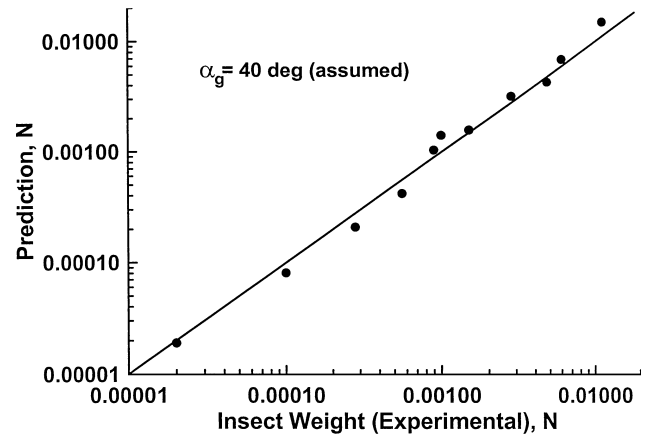
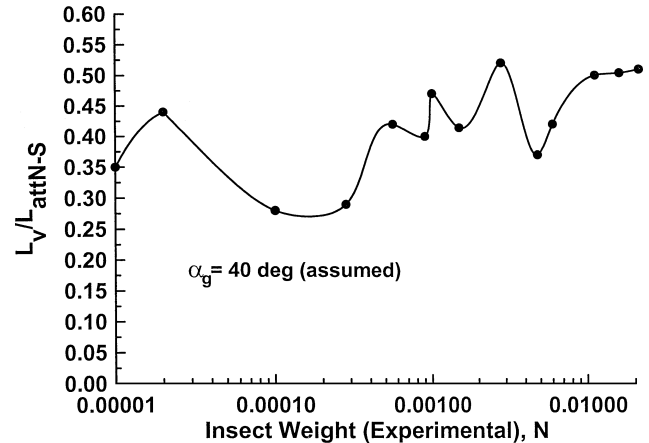
$$L_{\text{tot}} = qSK(c_r/R\phi) + \frac{[qSK(c_r/R\phi)]^{\frac{3}{2}}}{\cos(\alpha_g)^2 \sqrt{2\rho R^2 \phi \cos(\beta)}} \left(\frac{1}{\phi f R} \right) \quad (16)$$

To validate the functional relationship expressed by Eq. (16), the data sets presented by Weis-Fogh³ were used assuming $\beta = 0$ deg (see Table 1).

It would be expected that if Eq. (16) correctly relates the form and relative magnitudes of the attached and vortex lift components then values for K should be relatively constant, within the experimental accuracy. This is examined in Fig. 3. To evaluate K , L_{tot} is assumed equal to the animal weight. The angle of attack of an insect wing during a stroke cycle typically ranges from 30 to 50 deg, with lift showing moderate sensitivity to α_g in this range. Consequently, as a median value α_g was approximated as 40 deg. In Fig. 3 a logarithmic (base 10) scale is used for the insect weight because of the significant spread in the data. The results in Fig. 3 indicate that K is relatively invariant, with a mean value of $K_{\text{mean}} = 2.99$. Included in the figure is a 99.7% confidence interval. Predictions using $K = K_{\text{mean}} = 2.99$ are shown in Fig. 4. As would be expected, Eq. (16) shows good agreement with the experimental results.

The predicted ratio of vortex lift to attached flow lift (no leading-edge suction) is presented in Fig. 5. The levels of vortex lift range from approximately 27 to 50% of the attached flow lift. The vortex lift as a function of the total lift is shown in Fig. 6. The vortex lift is predicted to constitute approximately 23 to 34% of the total lift. Van den Berg and Ellington¹² conducted tests on a mechanical flapper designed to simulate the wing motions of the hawkmoth *Manduca sexta*. Using measurements of the rotational velocity of the vortex, they estimated the vortex lift that was developed. This was achieved using the Kutta–Joukowski equation:

$$L_v = \int_0^R \rho \omega r \Gamma v \, dr \quad (17)$$

**Fig. 3** Solution for constant K through evaluation of Eq. (16).**Fig. 4** Evaluation of predicted insect weight. Line through the origin indicates a perfect correlation.**Fig. 5** Computed ratio of wing vortex lift to attached flow lift with no leading-edge suction.

where ω is the time-averaged angular velocity of the wing and Γv is the sectional vortex circulation. Evaluation of Eq. (17) by van den Berg and Ellington¹² suggested that the vortex lift constituted 66% of the total lift developed in hover, which is approximately twice that predicted using Eq. (16), that is, 34% for this insect. To ascertain the validity of the computation method employed by van den Berg and Ellington, the same methodology was used for a case where the level of vortex lift was known. Two computations were performed: one using experimental results and the other an empirical relation to predict the circulation. Traub¹⁵ provides experimental data for the lift and vortex circulation developed over a 75-deg leading-edge sweep delta wing. The circulation was measured from crossflow

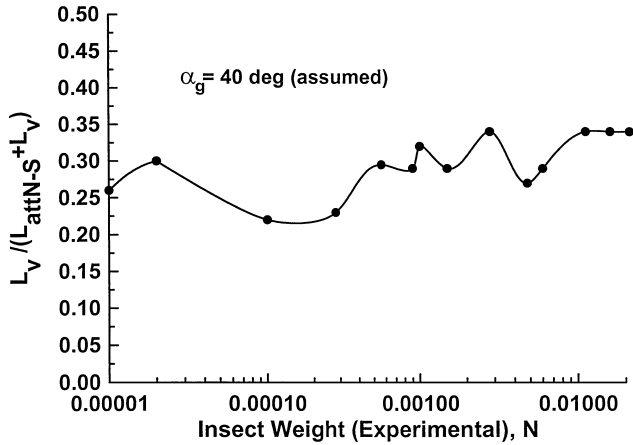


Fig. 6 Computed magnitude of the vortex lift as a function of the total lift.

surveys with a seven-hole probe. The second computation involved the use of an empirical relation to predict the circulation of the leading-edge vortex of a delta wing as given by¹⁶

$$\Gamma v = 4.63 U x \tan(\varepsilon)^{0.8} \tan(\alpha_g)^{1.2} \cos(\alpha_g) \quad (18)$$

Using the methodology of Eq. (17), the vortex lift associated with the circulation distribution expressed by Eq. (18) is given by

$$L_v = \int_0^{c_r} \frac{\rho U \cos(\Delta v) \Gamma v}{\cos(90 \text{ deg} - \Delta v)} dx \quad (19)$$

where $U \cos(\Delta v)$ is the velocity component normal to the leading-edge vortex. The level of vortex lift that is actually developed by the wing can be estimated using Polhamus' theory as verified by Er-El and Yitzhak.¹⁴ The experimentally observed vortex lift can thus be estimated as

$$L_{v\text{actual}} = \frac{1}{2} \rho U^2 \text{Swing} \pi \sin(\alpha_g)^2 \cos(\alpha_g) \quad (20)$$

The experimental data of Traub¹⁵ was measured on a 75-deg ($\varepsilon = 15$ deg) sweep delta wing with a root chord c_r of 0.375 m yielding $\text{Swing} = 0.03768 \text{ m}^2$ at $U = 20 \text{ m/s}$ and $\alpha_g = 20$ deg. The experimental data in this same reference indicated that the effective sweep angle of the leading-edge vortex was $\Delta v = 79.43$ deg. Using the experimental circulation data from Traub¹⁵ and substituting a curve fit of this distribution into Eq. (19) indicates that $2L_v/L_{v\text{actual}} = 1.85$. Note that there are two vortices on the wing; hence, the factor 2 in the numerator, the denominator already incorporates this. Evaluation of this ratio using Eqs. (18) and (19) yields $2L_v/L_{v\text{actual}} = 1.82$. Thus, both methods of calculation (empirical and experimental) indicate that the estimates of the vortex lift developed by the flapper (i.e., 66% of the total lift) are greatly exaggerated. These results indicate that only a fraction of the circulation of the vortex is effectively recovered as vortex lift when using the computational method of Eq. (19). Using van den Berg and Ellington's¹² estimate of 66% of the total lift consisting of vortex lift, but with a correctly scaled recoverable vortex lift (i.e., $L_{v\text{actual}}/2L_v$) gives $66\%/1.85 = 36\%$. This suggests that 36% of the total lift developed by the flapper was vortex lift. This is in good agreement with the estimate using the present theory [Eq. (16)], which yielded a value of 34% for the hawkmoth. This analysis does provide some experimental verification for the accuracy of Eq. (16).

The formulation of Eq. (14) does not include the wing incidence α_g . However, this can be incorporated as follows, by writing

$$K = C_{La2D} \sin(\alpha_g) \cos(\alpha_g)^2 \text{Corr} \quad (21)$$

where C_{La2D} is the two-dimensional lift-curve slope of the wing and Corr is a constant whose value must be established. For a flat-plate wing at a Reynolds number typical of an insect wing, Okamoto¹⁷ has shown that C_{La2D} can be assumed as $\approx 0.09/\text{deg}$. K ($=K_{\text{mean}}$) was

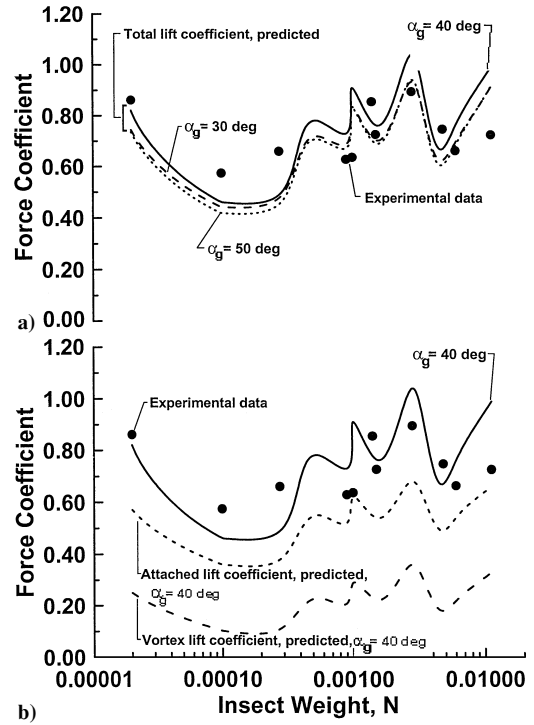


Fig. 7 Computed effect of wing incidence on the lift coefficient. a) Incidence effects and b) Lift constituents.

determined as 2.99 (for $\alpha_g = 40$ deg). For these values evaluation of Eq. (21) yields $\text{Corr} = 88$. Thus we can write

$$K = 88 C_{La2D} \sin(\alpha_g) \cos(\alpha_g)^2 \quad (22)$$

The effects of incidence are examined in Fig. 7a, which presents the total predicted lift coefficient for $\alpha_g = 30, 40$, and 50 deg, as well as the attached flow and vortex lift coefficients for $\alpha_g = 40$ deg (Fig. 7b). The coefficients were determined from Eqs. (14) and (15) with the aid of Eq. (11). Also included are experimental data for insect weight from Weis-Fogh.³ The data indicate that the effects of wing incidence are generally weak, a result that is also observed in experiment.⁷ This also supports the contention that attached flow mechanisms are responsible for the majority of the time-averaged lift. The change in the attached lift from $\alpha_g = 30$ to 50 deg is -16% (i.e., the attached flow lift reduces), while the change in the vortex lift is 41% . If the vortex lift was the dominant mechanism, the lift coefficient would show greater sensitivity to incidence.

Measurements⁵ on fruit flies have shown that loading is not uniform throughout the cycle and consists of various peaks, with associated lift coefficients approaching 3 (Ref. 1). This suggests that additional lift augmenting mechanisms must occur, that is, vortex lift alone is not sufficient to explain the instantaneous lift coefficient required by some insects at hover. The dynamic nature of the flow over insect wings can also lead to a delay of wing stall following the suppression of upper-surface boundary-layer separation as is observed on rapidly pitching wings. Transient attached flow lift coefficients greater than steady-state values can result. It is also likely that additional dynamic boundary-layer effects can be present and augment lift. Dickinson et al.¹ have suggested two additional lift augmentation mechanisms: rotational circulation and wake capture. Studies on a mechanical fly wing show that transient force peaks following stroke reversal can be caused by wake capture. A common simplification adopted in aerodynamic analysis is to discretize a lifting surface into discrete panels. Each panel can have a horseshoe-shaped vortex placed at the quarter-chord of the panel. The strength of these vortices is determined by applying the no-penetration condition, that is, fluid cannot physically penetrate the wing at control points. These control points are placed such that they yield the correct lift-curve slope for two-dimensional flow; they are placed at the $\frac{3}{4}$ chord of the discretised panel. Rotational circulation

is then the vortex strength required to enforce no penetration at the control point for a wing rotating or pitching about its spanwise axis. The further the rotation axis is from the control point the greater the rotational circulation. Similarly, if the wing is rotated about its $\frac{3}{4}$ chord (assuming the wing chord is replaced by one panel as in Weissinger lifting surface theory) it generates no rotational circulation. Wake capture is associated with use of the preexisting vortex field left over from the previous stroke to induce additional loading on the wing so enhancing lift. It is thus likely that certain insects use either or both of these effects to augment wing vortex and attached flow lift, although the last two mentioned are the dominant components. For lift data averaged over one stroke cycle, attached and vortex lift are sufficient to explain the loads generated for the animals investigated. Figure 7b shows that the magnitude of the attached flow and vortex lift coefficients are well within realizable levels with maximum time- and stroke-averaged force coefficients not exceeding 0.7.

Conclusions

A simple analytic expression is derived to estimate the stroke-averaged lift of a hovering insect based on geometric and kinematic data. The expression also allows for the decomposition of the total loading into its attached flow and vortex lift components assuming that the animal weight is already known. In addition, the methodology should prove useful for lift estimates in the conceptual design of biologically inspired microaerial vehicles. For the animals investigated, the vortex lift typically constituted 27–50% of the attached flow lift and approximately 23–34% of the total lift. As loading throughout the stroke cycle of an insect wing contains peaks where the instantaneous lift coefficient can approach 3, unsteady lift augmentation methods must be present.

Acknowledgments

The author would like to sincerely thank Murray Tobak of NASA Ames Research Center for his helpful comments. The author would also like to thank Ndaona Chokani for his helpful suggestions.

References

- ¹Dickinson, M. H., Lehmann, F. O., and Sane, S. P., "Wing Rotation and the Aerodynamic Basis of Insect Flight," *Science*, Vol. 284, June 1999, pp. 1954–1960.
- ²Ellington, C. P., van den Berg, C., Willmott, A. P., and Thomas, A. L. R., "Leading Edge Vortices in Insect Flight," *Nature*, Vol. 384, May 1996, pp. 626–630.
- ³Weis-Fogh, T., "Quick Estimates of Flight Fitness in Hovering Animals, including Novel Mechanisms for Lift Production," *Journal of Experimental Biology*, Vol. 59, 1973, pp. 169–230.
- ⁴Winter, H., "Stromungsvorgänge an Platten und Profilierten Körpern beil Kleinen Spannweiten," *Forschung auf dem Gebiete des Ingenieur-Wesens*, Vol. 6, 1935, pp. 67–71.
- ⁵Dickinson, M. H., and Gotz, K. G., "The Wake Dynamics and Flight Forces of the Fruit Fly *Drosophila Melanogaster*," *Journal of Experimental Biology*, Vol. 199, 1996, pp. 2085–2104.
- ⁶Wagner, H., "Über die Entdtehung des Dynamischen Auftriebes von Tragflügeln," *Zeitschrift für Angewandte Mathematik und Mechanik*, Vol. 5, 1925, pp. 17–35.
- ⁷Dickinson, M. H., and Gotz, K. G., "Unsteady Aerodynamic Performance of Model Wings at Low Reynolds Numbers," *Journal of Experimental Biology*, Vol. 174, 1993, pp. 45–64.
- ⁸Liu, H., Ellington, C. P., Kawachi, K., van den Berg, C., and Willmott, A. P., "A Computational Fluid Dynamic Study of Hawkmoth Hovering," *Journal of Experimental Biology*, Vol. 201, 1998, pp. 461–477.
- ⁹Polhamus, E. C., "Predictions of Vortex Lift Characteristics by a Leading Edge Suction Analogy," *Journal of Aircraft*, Vol. 8, No. 4, 1971, pp. 193–198.
- ¹⁰Smith, M. J. C., Wilkin, P. J., and Williams, M. H., "The Advantages of an Unsteady Panel Method in Modeling the Aerodynamic Forces on Rigid Flapping Wings," *Journal of Experimental Biology*, Vol. 199, 1996, pp. 1073–1083.
- ¹¹Ellington, C. P., "The Aerodynamics of Hovering Insect Flight. V. A Vortex Theory," *Philosophical Transactions of the Royal Society of London*, Pt. B, Vol. 305, 1984, pp. 115–144.
- ¹²van den Berg, C., and Ellington, C. P., "The Three-Dimensional Leading-Edge Vortex of a 'Hovering' Model Hawkmoth," *Philosophical Transactions of the Royal Society of London*, Pt. B, Vol. 305, 1997, pp. 329–340.
- ¹³Traub, L. W., "Prediction of Vortex Breakdown and Longitudinal Characteristics of Swept Slender Planforms," *Journal of Aircraft*, Vol. 34, No. 3, 1997, pp. 353–359.
- ¹⁴Er-El, J., and Yitzhak, Z., "Experimental Examination of the Leading-Edge Suction Analogy," *Journal of Aircraft*, Vol. 25, No. 3, 1988, pp. 195–199.
- ¹⁵Traub, L. W., "Effects of Anhedral and Dihedral on a 75-deg Sweep Delta Wing," *Journal of Aircraft*, Vol. 37, No. 2, 2000, pp. 302–312.
- ¹⁶Traub, L. W., "Prediction of Delta Wing Leading-Edge Vortex Circulation and Lift-Curve Slope," *Journal of Aircraft*, Vol. 34, No. 3, 1997, pp. 450–452.
- ¹⁷Okamoto, M., Yasuda, K., and Azuma, A., "Aerodynamic Characteristics of the Wings and Body of a Dragonfly," *Journal of Experimental Biology*, Vol. 199, 1996, pp. 281–294.